

Suction surface:

$$B = 0.47078$$

$$C = -0.12464$$

$$D = -29.63788$$

$$E = 10.06706$$

$$F = 0$$

$$x^2 + (0.47078)xy + (-0.12464)y^2 + (-29.63788)x + (10.06706)y = 0$$

Pressure surface:

$$B = 0.17614$$

$$C = -30.39820$$

$$D = 14.59569$$

$$E = 13.26829$$

$$x^2 + (0.17614)y^2 + (-30.39820)x + (14.59569)y + 13.26829 = 0$$

Once the values for the coefficients have been determined, the curve properties are calculated routinely.

### Reference

<sup>1</sup> Deich, M. E., "Flow of gas through turbine latices," English transl., NACA TM 1393, Washington, D. C. (May 1956).

# Design Optimization of Aircraft Structures with Thermal Gradients

LLOYD E. HACKMAN\* AND JAMES E. RICHARDSON†  
*North American Aviation, Inc., Columbus, Ohio*

A technique of optimizing a structure subjected to a thermal gradient has been developed. The derivation of optimization equations is demonstrated for three types of basic structure: 1) a honeycomb compression panel, 2) a skin-stringer compression element, and 3) an I-beam section. The optimization on these typical structural elements is performed maintaining the interdependency of the structural configuration and the temperature distribution. The procedures also maintain such variables as material properties and a nonlinear stress-strain relation. The complexity of the applied stress and allowable equations has dictated a change in approach of the optimization problem to one of allowable and applied strains rather than allowable and applied stresses. It must be concluded from the results of this optimum design study that it is feasible to account for thermal stress and temperature effects in the preliminary design stages of an aircraft structure.

## Nomenclature

$A$	= defined by Eq. (2)
$A_S, A_T, A_L,$ $A_F, A_n$	= area, in. <sup>2</sup>
$a$	= width of panel, loaded edge, in.
$b$	= length of panel, unloaded edge, in.
$b_s$	= stringer spacing, in.
$C$	= core depth, in.
$C_s$	= effective area coefficient
$c_1, c_2, c_3, c_4$	= edge fixity constants, Ref. 1
$CL$	= cord length, in.
$E$	= Young's modulus, psi
$e$	= strain, in./in.
$F$	= panel buckling constant
$F_{ci}$	= intercell buckling stress, psi
$F_c$	= compression stress, psi
$F_t$	= tension stress, psi
$F_y$	= yield stress, psi
$G_c'$	= effective core shear modulus, psi
$h$	= stringer, depth, in.
$K$	= panel buckling constant
$K_T$	= thermal constant, °F-in.
$L$	= panel buckling constant
$L_c$	= column length, in.
$m$	= Ramberg-Osgood coefficient

$M_u$	= applied bending moment, in./lb
$P$	= applied axial load, lb/in.
$P_A, P_{cc}, P_s$	= axial load, lb
$Q$	= applied shear load, lb
$S$	= core cell size, in.
$t$	= thickness, in.
$t_f$	= honeycomb panel facing, in.
$t_c$	= core foil thickness, in.
$T$	= temperature, °F
$T_B$	= boundary-layer temperature, °F
$V_x, V_y$	= core shear stiffness parameter
$y, y_n$	= element distance from a given axis, in.
$\mu$	= Poisson's ratio
$\alpha$	= coefficient of expansion, in./°F-in.

## Subscripts

$b$	= stringer
$c$	= core
$cc$	= crippling
$cR$	= critical buckling stress
$cy$	= compression yield
$f$	= facing
$L$	= lower
$n$	= generalize element number
$R$	= effective modulus
$s$	= secant, skin
$T$	= tangent
$u$	= upper, ultimate
$w$	= web
$x$	= component in $x$ direction
$y$	= component in $y$ direction
1	= hot facing of honeycomb panel
2	= cold facing of honeycomb panel

Presented as Preprint 63-9 at the IAS 31st Annual Meeting, New York, January 21-23, 1963; revision received September 27, 1963.

\* Specialist, Structural Mechanics Research and Development Section. Member AIAA.

† Engineer, Structural Mechanics Research and Development Section; now in Structures Group, Liquid Rocket Plant, Aerojet General, Sacramento, Calif.

APPROACHING the optimization of structures with thermal gradients by a conventional manner yielded a maze of complex equations. Therefore, a new approach was sought. Since it is known that the strain from the axial load is constant across the section and that the thermal strains are dependent only on the constants, temperature, and  $\alpha$ , the strain on any element or elements can be determined if the total strain on any one element is assumed. Thus, from several assumed strain distributions, the allowable strain equations, and the equilibrium equations, several compression panel configurations can be determined. These configurations can then be compared to determine the minimum-weight

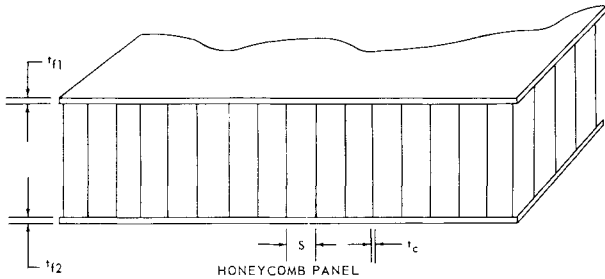


Fig. 1 Honeycomb panel.

panel configuration. If bending enters the problem, an expression for the bending strain may be included by assuming a maximum bending strain on an element with a straight-line distribution between elements. Thus, assumed bending strain is iterated until bending equilibrium is achieved. Again several configurations are computed using different total strains on a given element in order to determine the minimum-weight configuration.

The following sections discuss the derivation of the strain equations, equilibrium equations, allowable strain equations, and weight equations necessary to determine the optimum design. The procedures for combining these equations and developing a final minimum-weight design configuration are also discussed in detail. Examples of the successful application of these methods are presented in the paper as design curves.

### Honeycomb Compression Panels

In this section we shall consider the method derived for the fixed-load honeycomb panel (Fig. 1). The design method has been derived for thermal gradients dependent on facing thickness, core density, and core depth. The facing temperatures have been expressed in an empirical tabular form as functions of the configuration parameters, so that a minimum amount of time is expended computing temperatures. However, since the final temperature and the configuration are interdependent, an iterative process is required in order to determine the final balanced design condition.

The honeycomb compression panel with a fixed load is designed to satisfy three failure modes: general panel buckling, face wrinkling, and intercell buckling. The general buckling allowable load<sup>1</sup> as used in the following derivation is a function of two unequal facing thicknesses with different material properties, core depth, core density, edge fixity conditions, and panel size. This equation can be written as follows:

$$P = \frac{P_M A H^2}{a^2} \quad (1)$$

$$A = \frac{\pi^2 t_{f1} t_{f2} E_1 E_2}{(1 - \mu^2)(t_{f1} E_1 + t_{f2} E_2)} \equiv \frac{\pi^2 Y}{(1 - \mu^2)} \quad (2)$$

$$H = \left( C + \frac{t_{f1} + t_{f2}}{2} \right) \equiv C + X \quad (3)$$

$$P_M = \frac{K + [(V_x/c_4) + V_y]F}{1 + L + (V_x V_y/c_4)F} \quad (4)$$

$$K = c_1 + 2c_2 + c_3 \quad (5)$$

$$F = c_1 c_3 - c_2^2 + \frac{1 - \mu}{2} c_2 K \quad (6)$$

$$L = \left( c_1 + \frac{1 - \mu}{2} c_2 \right) \frac{V_x}{c_4} + \left( c_3 + \frac{1 - \mu}{2} c_2 \right) V_y \quad (7)$$

The core shear parameters are

$$V_y = K_1 Y C / G_{cy}' \quad V_x = K_1 Y C / G_{cx}' \quad (8)$$

where

$$K_1 = \frac{\pi^2}{a^2(1 - \mu^2)} \quad Y = \frac{t_{f1} t_{f2} E_1 E_2}{(t_{f1} E_1 + t_{f2} E_2)} \quad (9)$$

$$G_{cx}' = G_{cy}'/2 \text{ for hexcell core} \quad (10)$$

$$G_{cx}' = G_{cy}' \text{ for square cell core} \quad (11)$$

The face-wrinkling mode of failure is primarily a function of the core density and facing modulus. The allowable facing stress is expressed as follows:

$$F_{cw} = 0.5[0.066(t_c/S)^2 G_c E_c (E_s + 3E_T)]^{1/3} \quad (12)$$

It must be noted at this point, however, that the facing moduli,  $E_s$  and  $E_T$ , are functions of  $F_{cw}$ . In such a case, the Ramberg-Osgood stress-strain relation must be used. Intercell buckling is also dependent upon the Ramberg-Osgood strain relation, along with facing thickness and cell size. The allowable intercell buckling face stress is written as follows:

$$F_{ci} = 0.9E_R \left( \frac{t_f}{S} \right)^{3/2} = \frac{1.8EE_T}{E + E_T} \left( \frac{t_f}{S} \right)^{3/2} \quad (13)$$

With the allowable equations (1, 12, and 13), the design of a honeycomb compression panel can be accomplished. The requirements of the design for this derivation have included a temperature gradient, as well as the axial compression load. The applied stress under these conditions can be expressed as follows:

$$F_c \text{ applied} = -\alpha E \Delta T + (1/A_F) \Sigma \alpha E \Delta T \Delta A_F - (P/\Sigma \Delta A_F) \quad (14)$$

Because of the two facings being at different temperatures and thus having different material properties and stress levels, an effective area of each element must be used. No bending relief stress is used in this analysis, since it is assumed that the panels are restrained in bending by adjacent structure. Equation (14) can now be rewritten as follows:

$$F_c \text{ applied} = -\alpha_1 E_{s1} (T_1 - T_B) + \frac{\alpha_1 E_{s1} (T_1 - T_B) t_{f1} + \alpha_2 E_{s2} (T_2 - T_B) t_{f2}}{t_{f1} + (E_{s2}/E_{s1}) t_{f2}} - \frac{P}{t_{f1} + (E_{s2}/E_{s1}) t_{f2}} \quad (15)$$

For the design of the minimum-weight panel, the allowable face wrinkling and general panel buckling stresses will be equal to the applied-load stress. Therefore, a relation for core density ( $t_c/S$ ) can be derived by combining Eqs. (12) and (15) and solving for  $t_c/S$ :

$$\frac{t_c}{S} = \frac{11.0(F_c \text{ applied})^{3/2}}{G_c E_c (E_{s1} + 3E_{T1})^{1/2}} \quad (16)$$

Another parameter that must be determined is the core depth  $C$ . A cubic expression for  $C$  may be derived directly

from the general buckling equation (1) by substituting (2-4, 8, 10, and 11) and following by algebraic manipulations to the form

$$C^3 \left[ F Y \left( \frac{K_1^2}{G_{cx}' c_4} + \frac{K_1^2}{G_{cy}'} \right) \right] + C^2 \left[ K_1 K + 2 X F Y \left( \frac{K_1^2}{G_{cx}' c_4} + \frac{K_1^2}{G_{cy}'} \right) - \frac{P K_1^2 F Y}{G_{cx}' G_{cy}' c_4} \right] + C \left[ 2 X K_1 K + X^2 F Y \left( \frac{K_1^2}{G_{cx}' c_4} + \frac{K_1^2}{G_{cy}'} \right) - K_1 P \left( \frac{c_1 + [(1 - \mu)/2] c_2}{c_4 G_{cx}'} + \frac{c_3 + [(1 - \mu)/2] c_2}{G_{cy}'} \right) \right] + X^2 K_1 K - \frac{P}{Y} = 0 \quad (17)$$

No further reduction of Eq. (17) was attempted, since the solution of the cubic will be performed on a digital computer.

All equations (13, 16, and 17) for the design of a honeycomb panel in compression have now been presented. The following design procedure has been derived to compute the minimum-weight (optimum) configuration under the stipulated conditions. The basic approach has been changed from one of stress as used in the past to one of strain. By assuming the total strain on one facing of the panel, the strain can be computed for the other facing. The strain on the second facing is expressed as follows:

$$e_2 = e_1 + \alpha(T_1 - T_2) \quad (18)$$

This equation is valid, since it has been assumed that no bending occurs in the panel.

At this point an arbitrary facing thickness  $t_{f1}$  is also assumed. With this assumed value of  $t_{f1}$  an initial estimate of the facing temperatures is computed. This initial estimate is made with a very simple equation:

$$T = (K_i/t_{f1}) + T_B \quad (19)$$

Knowing  $e_1$  and  $e_2$  and the temperature of the facings, the facing stress  $F$  can be computed using the Ramberg-Osgood equation in an iterative process:

$$e = (F/E) [1 + \frac{3}{m} (F/F_y)^{m-1}] \quad (20)$$

The yield stress  $F_y$  is obtained from material properties at temperature.

With known  $t_{f1}$  and facing stresses  $F_{c1}$  and  $F_{c2}$ , the second facing thickness  $t_{f2}$  can be computed as a function of the applied load  $N$ :

$$t_{f2} = (N - t_{f1} F_{c1})/F_{c2} \quad (21)$$

Two other parameters,  $t_c/S$  and  $C$ , remain to be determined to complete the panel configuration; they can be determined from Eqs. (15) and (17), respectively. With the final determination of panel configuration for the given load, temperature,  $t_{f1}$ , and  $e_1$ , a new estimate for temperature distribution

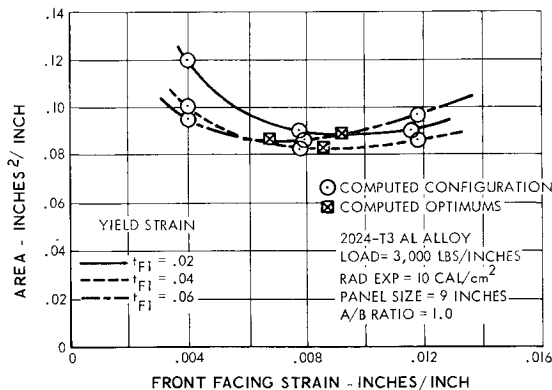


Fig. 2 Optimum strain selection.

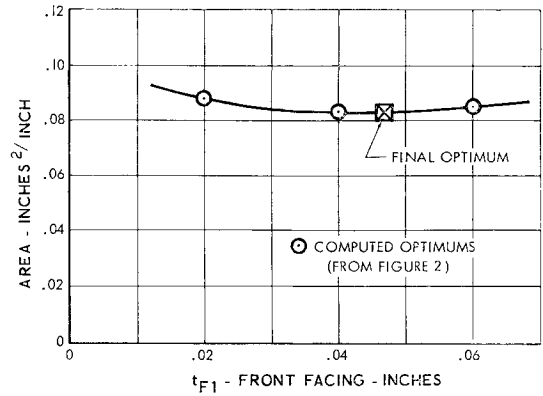


Fig. 3 Optimum  $t_{f1}$  selection.

can be made with much greater accuracy, following the method from Ref. 2.

The process of estimating the temperature and recomputing the panel configuration as described is repeated until temperature convergence is achieved. The area or relative weight of this configuration can be determined as follows:

$$A_T = t_{f1} + t_{f2} + K(t_c/S)C \quad (22)$$

where  $K = 2$  for square cell, 3 for Hexcell.

With a compatible panel configuration determined for the assumed strain  $e_1$  and facing thickness  $t_{f1}$ , another strain  $e_1$  will be assumed. A compatible panel configuration is then determined for this assumed strain also. This process is repeated for a third time so that there are three different configurations. The strain at which the minimum weight configuration occurs (Fig. 2) can now be determined by fitting an equation for area vs  $e_1$  through the three points, differentiating the equation and setting it equal to zero. The  $e_1$  that satisfies  $dA_T/de_1 = 0$  is the strain for the minimum weight (or area) configuration.

This whole process is repeated for two other values of  $t_{f1}$  to establish three optimum  $e_1$  configurations as a function of  $t_{f1}$  (Fig. 2). The "absolute optimum" can now be determined by fitting an equation for the area through the three computed points as a function of  $t_{f1}$  (Fig. 3), setting the derivative ( $dA_T/dt_{f1}$ ) equal to zero, solving this equation for the optimum  $t_{f1}$ , and determining the configuration compatible with the optimum  $t_{f1}$ .

### Integral Skin-Stringer Panels

This section considers the optimum design of an integral skin-stringer panel with a thermal gradient under a given axial load  $P$ , as shown in Fig. 4a. For the purpose of analysis, only one  $T$ -section will be considered (Fig. 4b). The temperatures of the skin and stringers are assumed to be functions of the skin thickness and stringer depth, respectively. It is assumed that, for an optimum design, the stringer will be stable, and the skin will be subject to local buckling.

For a given stringer spacing  $b_s$  and skin thickness  $t_s$ , the temperature of the skin  $T_s$  may be determined. In this case, the skin temperature is assumed to be related to the skin thickness by

$$T_s = (K_T/t_s) + T_B \quad (23)$$

At this point, a value of the skin strain  $e_s$  must be assumed, along with a value of the stringer depth  $h$ . The stringer temperature may now be determined by

$$T_b = (K_T/\frac{1}{2}h) + T_B \quad (24)$$

Since the panel is assumed to be restrained in bending, the stringer strain  $e_b$  may now be calculated by

$$e_b = e_s + \alpha(T_s - T_b) \quad (25)$$

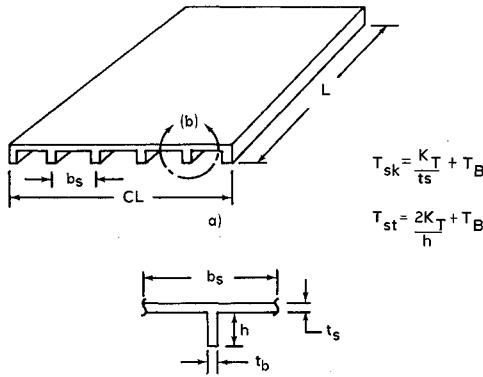


Fig. 4 Integral skin-stringer panel.

At this point, the skin stress  $f_s$  and the stringer  $f_b$  associated with the strains  $e_s$  and  $e_b$  may be calculated by the Ramberg-Osgood Eq. (20). The stringer thickness  $t_b$  may be determined by combining the buckling equation and the Ramberg-Osgood equation:

$$e_{crs} = e_{cb} = K_{cb}(t_b/h)^2 = F_{cys}/0.7E_b \quad (26)$$

where  $e_{cy}$  is the compression yield strain of the stringer and  $K_{cb}$  is the buckling coefficient ( $K_{cb} = 0.385$  for one edge free), and  $F_{cys}$  is the compression yield stress of the stringer. Therefore,

$$t_b = h(F_{cys}/0.7E_b K_{cb})^{1/2} \quad (27)$$

Since the skin is allowed to buckle, the effective area coefficient  $C_s$  must be calculated. From Sec. 7-5 for Ref. 5, the approximate value of  $C_s$  is

$$C_s = (e_{crs}/e_s)^{1/2} \quad e_s > e_{crs} \quad (28)$$

$$C_s = 1 \quad e_s \leq e_{crs}$$

where  $e_{crs} = K_{cs}(t_s/b_s)^2$ . The axial load equilibrium equation may be written and solved for  $h$ :

$$h = \frac{P_s - f_s t_s CL C_s}{f_b [(CL/b_s) + 1] t_b} \quad (29)$$

The value of  $h$  calculated is compared with the value of  $h$  originally assumed, and the process is iterated on  $h$ . The panel must now be checked to see if it is critical as a column. The critical load  $P_{cc}$  may be determined by

$$P_{cc} = \Sigma f_n A_n C_n = f_s t_s CL C_s + F_{cys} t_b h [(CL/b_s) + 1] \quad (30)$$

Note that  $f_b$  has been set equal to  $F_{cys}$  for a column cutoff stress.

The allowable column load  $P_A$  may be determined from Sec. 14.6 of Ref. 3:

$$P_A = P_{cc} \left[ 1 + \frac{P_{cc}(L_e/\rho)^2}{4\pi^2 E \Sigma A_n} \right] \quad (31)$$

or

$$P_A = P_{cc} \left[ 1 + \frac{P_{cc} L_e^2 (t_s b_s C_s + t_b h)}{4\pi^2 E_b [t_s CL C_s + (CL/b_s + 1) t_b h] \{ \bar{y}^2 t_s b_s C_s (E_s/E_b) + t_b h [(t_s + h)/2 - \bar{y}]^2 + t_b h^3/12 \}} \right] \quad (32)$$

The distance to the neutral axis  $\bar{y}$  may be located by

$$\bar{y} = \frac{\Sigma E_n A_n y_n}{\Sigma E_n A_n} = \frac{E_s t_s h (h + t_s)/2}{E_s t_s b_s + E_b t_b h} \quad (33)$$

Next, a new value of skin strain  $e_s$  is chosen, and the entire procedure just outlined is repeated. After several values of  $e_s$  have been chosen, a plot is made of  $e_s$  vs total area  $A_T$ , where

$$A_T = t_s CL + (CL/b_s + 1) t_b h \quad (34)$$

A plot also is made of  $e_s$  vs  $P_A$ . At the point where the col-

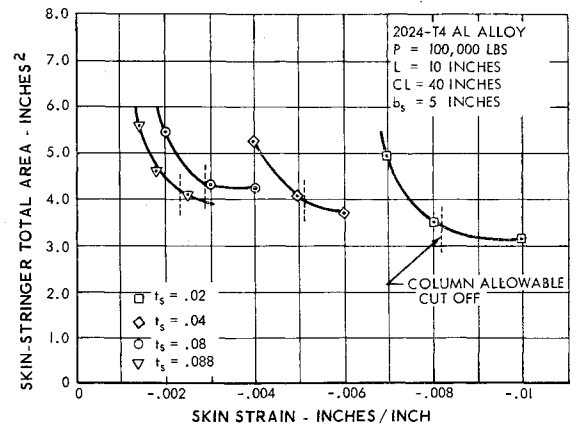
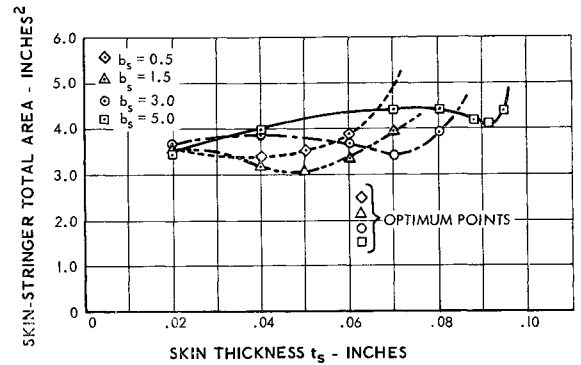


Fig. 5 Optimum strain selection.

Fig. 6 Optimum  $t_s$  selection.

umn's allowable load  $P_A$  is equal to the applied load  $P_s$ , the curve  $e_s$  vs  $A_T$  is cut off, because strains larger than this produce column buckling (see Fig. 5). The cutoff value of  $e_s$  is the optimum skin strain for a given skin thickness  $t_s$  and stringer spacing  $b_s$ . Next, a new value of skin thickness  $t_s$  is chosen, and the foregoing procedure is repeated. After several values of  $t_s$  have been chosen, a plot is made of  $t_s$  vs  $A_T$  (Fig. 6). The minimum of this curve gives the optimum skin thickness for a given stringer spacing  $b_s$ . Finally, several other values of stringer spacing  $b_s$  are chosen, and the steps previously outlined are repeated. A plot is made of  $b_s$  vs  $A_T$  (Fig. 7). The minimum of this curve is then the final optimum configuration.

The allowable load for the optimum configuration was determined by the methods outlined in Ref. 4. It was found that the allowable load of the  $T$ -section checked very closely with the applied load (less than 3% difference). This close approximation between the allowable and applied load indicates the accuracy of the design method.

### I-Beams

An  $I$ -beam is assumed to be loaded, as shown in Fig. 8, where

$M_u$  is an applied moment (inch-pounds) and  $Q$  is an applied shear force (pounds) and is assumed to be unrestrained in bending. The temperature of the upper skin element  $s$  is assumed to be a function of the skin thickness. The temperature of the web element  $T_w$  and the lower cap element  $T_L$  are assumed to remain constant.

According to Gatewood and Gehring,<sup>4</sup> the strain on any element  $n$  may be written as

$$e_n = -\alpha_n T_n + (e_{ap} + e_p + e_T) + (y_n/c)(K_{ap} + K_p + K_T) \quad (35)$$

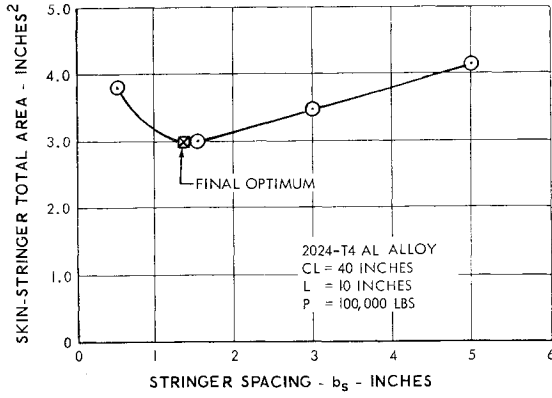


Fig. 7 Optimum stringer spacing selection.

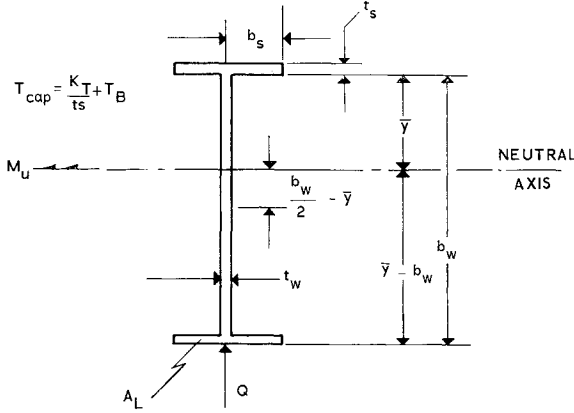


Fig. 8 I-beam.

where  $y_n$  is the distance from the centroid of the element  $n$  to the neutral axis, and  $c$  is the maximum value of  $y_n$ .

The strain equations of the web and lower cap may then be written in terms of  $e_s$  as

$$e_w = e_s + \alpha(T_s - T_w) + \frac{1}{2}e_{Lb} \quad (36)$$

$$e_L = e_s + \alpha(T_s - T_L) + e_{Lb} \quad (37)$$

where  $e_{Lb} = (y_n/c)(K_{ap} + K_p + K_T)$  for the lower cap.

First, a value of the skin thickness  $t_s$  is assumed, and the skin temperature  $T_s$  determined from Eq. (23). Values are now assumed for both  $e_s$  and  $e_{Lb}$ . The strains  $e_w$  and  $e_L$  may now be calculated by Eqs. (36) and (37). The stresses associated with these strains  $f_s$ ,  $f_w$ , and  $f_L$ , along with the secant moduli  $E_{ss}$ ,  $E_{sw}$ , and  $E_{sL}$ , may be determined from the Ramberg-Osgood stress-strain relationship, Eq. (20). The skin stress  $f_s$  is assumed to have a maximum value of  $F_{cy}$ .

The web is designed to carry the average axial strain  $e_w$  and shear strain without buckling. The allowable shear stress  $F_{scr}$  can be expressed as follows:

$$F_{scr} = K_{ws}(t_w/b_w)^2 E_{Tw} \quad (38)$$

where  $K_{ws}$  is the shear buckling coefficient and  $E_{Tw}$  is the tangent modulus. The allowable axial stress is expressed as

$$F_{cr} = K_w(t_w/b_w)^2 E_{Tw} \quad (39)$$

where  $K_w$  is the compression buckling coefficient. The applied shear stress and axial stresses are

$$f_s = Q/t_w b_w \quad (40)$$

$$f_w = e_w E_{sw} \quad (41)$$

These values are combined in the shear and axial load combined stress equations to derive an expression for  $t_w$  as follows:

$$\pm (f_w/F_{cr})^2 + (f_s/F_{scr})^2 = 1 \quad (42)$$

The sign of the first term of Eq. (42) depends on the stress  $f_s$ . If the web is in compression the sign is plus, and if the web is in tension the sign is minus.

Solving for  $t_w$ ,

$$t_w^6 \pm (e_w b_w^2 / K_w)^2 t_w^2 - (Q b_w / K_{ws} E_{Tw})^2 = 0 \quad (43)$$

Equation (43) can now be solved for  $t_w$ . The lower cap area  $A_L$  may be determined by

$$A_L = M_u / b_w F_{tL} \quad (44)$$

where  $F_{tL}$  is the ultimate tension stress of the lower cap.

The axial load equilibrium equation may now be written as

$$2b_s t_s e_s E_{ss} + e_w b_w t_w E_{sw} + e_L A_L E_{sL} = 0 \quad (45)$$

Solving Eq. (45) for  $2b_s t_s$ ,

$$2b_s t_s = A_s = \frac{-e_w b_w t_w E_{sw} - e_L A_L E_{sL}}{e_s E_{ss}} \quad (46)$$

where  $A_s$  is the area of the upper cap.

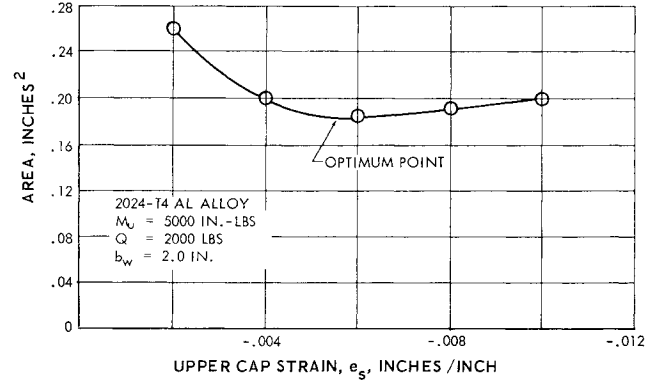


Fig. 9 Optimization curve.

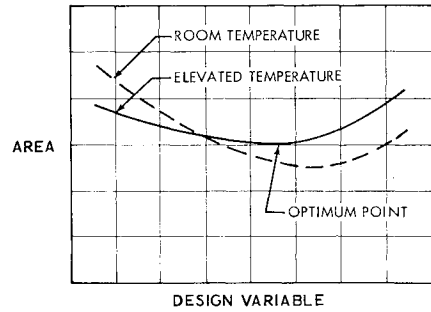


Fig. 10 Superposition of room and elevated temperature optimization curves.

Using the upper skin as a reference axis, the distance to the neutral  $\bar{y}$  axis may be calculated by

$$\bar{y} = \frac{(b_w^2/2)t_w E_{sw} + b_w A_L E_{sL}}{A_s E_{ss} + b_w t_w E_{sw} + A_L E_{sL}} \quad (47)$$

The moment equilibrium equation may be written as

$$M_u = -e_s E_{ss} A_s \bar{y} - e_w E_{sw} b_w t_w (\bar{y} - b_w/2) - e_L E_{sL} A_L (\bar{y} - b_w) \quad (48)$$

Substituting Eqs. (36) and (37) into Eq. (48) for  $e_L$  and  $e_w$  and solving for  $e_{Lb}$ ,

$$e_{Lb} = \frac{M_u + e_s E_{ss} A_s \bar{y} + E_{sw} t_w b_w (\bar{y} - b_w/2) [e_s + \alpha(T_s - T_w)]}{-E_{sL} A_L (\bar{y} - b_w) - \frac{1}{2} E_{sw} t_w b_w (\bar{y} - b_w/2)} + \frac{[e_s + \alpha(T_s - T_L)] E_{sL} A_L (\bar{y} - b_w)}{-E_{sL} A_L (\bar{y} - b_w) - \frac{1}{2} E_{sw} t_w b_w (\bar{y} - b_w/2)} \quad (49)$$

This value of  $e_{Lb}$  is then compared with the original value of  $e_{Lb}$  assumed and the process iterated on  $e_{Lb}$ .

The upper skin is assumed to remain stable for an optimum design. Therefore,

$$e_s = -K_{cs}(t_s/b_s)^2 \quad b_s = A_s/2t_s \quad (50)$$

or

$$t_s = (A_s/2)^{1/2}(-e_s/K_{cs})^{1/4} \quad (51)$$

This value of  $t_s$  is then compared with the original value of  $t_s$  assumed and the process iterated on  $t_s$ .

Next a new value of the skin strain  $e_s$  is chosen, and the entire procedure outlined previously is repeated. After several values of  $e_s$  are chosen, a plot is made of  $A_T$  vs  $e_s$  (Fig. 9), where  $A_T$  is the total area of the  $I$ -beam and is calculated by

$$A_T = A_s + b_w t_w + A_L \quad (52)$$

Also, a plot must be made with room temperature values to determine the critical area. The minimum of this composite curve (combination of elevated and room temperature curves) is the point of optimum design. A typical example is shown in Fig. 10.

### Restrictions and Applications

Optimization methods have been developed for honeycomb panels, integral skin-stringer panels, and  $I$ -beams subjected to variable temperature gradients. However, as with all methods, certain restrictions and limitations must be imposed.

For example, the  $I$ -beam optimization method is for a variable mold line, since the beam depth  $b_w$  is the distance between centroids of the upper and lower caps. The mold line varies, depending on the skin thickness, but this variation is small, so that a good approximation may be made of the

optimum design. If the design limits permit, optimum depth  $b_w$  can be found for the  $I$ -beam by extending the method previously outlined to include a variable depth  $b_w$ .

The optimum design at elevated temperatures may not be optimum at room temperature and may, in fact, not be able to sustain the applied load at room temperature. Therefore, the methods presented here must be used to determine if the structure is indeed critical at room temperature. A plot may be made of the room temperature optimum curve superimposed upon the elevated temperature optimum curve as shown in Fig. 10. The intersection of these two curves is the optimum design point when both room temperature and elevated temperature are considered, except when the minimum of one of the curves lies inside the envelope described by the two curves.

This principle of superposition of optimum curves may be extended to other parameters produced by different conditions and a design envelope established to determine an optimum structure that will satisfy all of the conditions imposed upon it.

### References

- 1 Ericksen, W. S. and March, H. W., "Compressive buckling of sandwich panels having dissimilar facings of unequal thickness," Forest Products Lab., Forest Service, U. S. Dept. Agriculture 1583-B (1958).
- 2 Holmboe, K. C., "An analysis of the thermal response of bonded aluminum honeycomb structure to nuclear detonations," North American Aviation Inc., NA60H-192 (1960), pp. 40-43.
- 3 Perry, D. J., *Aircraft Structures* (McGraw-Hill Book Co. Inc., New York, 1950), Sec. 14.6.
- 4 Gatewood, B. E. and Gehring, R. W., "Allowable axial loads and bending moments for inelastic structures under non-uniform temperature distribution," J. Aerospace Sci. 29, 513-520 (1962).
- 5 Gatewood, B. E., *Thermal Stresses* (McGraw-Hill Book Co., Inc., New York, 1957), Sec. 7-5.

## Low-Altitude, High-Speed Handling and Riding Qualities

RALPH C. A'HARRAH\*

*North American Aviation, Inc., Columbus, Ohio*

The results of a combined flight and ground-based dynamic flight simulator study of the handling and riding qualities problems associated with low-altitude, high-speed flight are presented in this paper. Wide variations of the longitudinal stability and control characteristics, which can be considered representative of current and future strike aircraft, were pilot evaluated. The influence of these stability and control characteristics, as well as the effects of low-altitude turbulence on the pilots' terrain-following performance, were measured. The results of this investigation are presented in terms of iso-opinion and iso-performance boundaries defining the desired and required combinations of stability and control parameters for low-altitude, high-speed flight. These acceptance boundaries are significantly different from the boundaries presently defined in the Military Specifications. Combinations of vehicle and control system characteristics, which tend to become unstable when coupled with the pilots' response (i.e., pilot-induced oscillations), have been defined.

### Nomenclature

$A$	= numerator time constant in pitch acceleration-gust velocity equation, sec
$D_{sp}$	= $s^2 + 2\zeta\omega_n s + \omega_n^2$ , 1/sec <sup>2</sup>
$D_{sp}'$	= $(s^2/\omega_n^2) + (2\zeta s/\omega_n) + 1$

$f_n$	= natural frequency, cps
$F_s$	= stick force, lb
$F_s/n_z$	= stick force per unit load factor, lb/g
$g$	= acceleration due to gravity, 32.2 ft/sec <sup>2</sup>
$h$	= altitude, ft
$\ddot{h}$	= climb acceleration, ft/sec <sup>2</sup>
$h_e$	= altitude error, ft

Presented at the AIAA Summer Meeting, Los Angeles, Calif., June 17-20, 1963; revision received December 11, 1963. This paper presents research effort sponsored and directed by the Stability and Control Unit of the Bureau of Naval Weapons under Contract N0w 61-0699-d.

\* Principal Engineer, Flight Mechanics Research, Columbus Division.